Journal of Controlled Release 172 (2013) 862–871

Contents lists available at ScienceDirect

Journal of Controlled Release

journal homepage: www.elsevier.com/locate/jconrel

In vivo real-time monitoring system of electroporation mediated control of transdermal and topical drug delivery

Tanja Blagus [a], Bostjan Markelc [a], Maja Cemazar [a,b], Tina Kosjek [c], Veronique Preat [d], Damijan Miklavcic [e], Gregor Sersa [a,*]

[a] Department of Experimental Oncology, Institute of Oncology Ljubljana, Zaloska 2, SI-1000 Ljubljana, Slovenia
[b] Faculty of Health Sciences, University of Primorska, Polje 42, SI-6310 Izola, Slovenia
[c] Department of Environmental Sciences, Jozef Stefan Institute, Jamova 39, SI-1000 Ljubljana, Slovenia
[d] Louvain Drug Research Institute, Pharmaceutics and Drug Delivery, Université Catholique de Louvain, Avenue E. Mounier, 73 B1.73.12, 1200 Brussels, Belgium
[e] University of Ljubljana, Faculty of Electrical Engineering, Trzaska cesta 25, SI-1000 Ljubljana, Slovenia

ARTICLE INFO

Article history:
Received 6 August 2013
Accepted 27 September 2013
Available online 7 October 2013

Keywords:
Electroporation
Transdermal drug delivery
Topical drug delivery
Multi-array electrodes
Monitoring system
Controlled delivery

ABSTRACT

Electroporation (EP) is a physical method for the delivery of molecules into cells and tissues, including the skin. In this study, in order to control the degree of transdermal and topical drug delivery, EP at different amplitudes of electric pulses was evaluated. A new *in vivo* real-time monitoring system based on fluorescently labeled molecules was developed, for the quantification of transdermal and topical drug delivery. EP of the mouse skin was performed with new non-invasive multi-array electrodes, delivering different amplitudes of electric pulses ranging from 70 to 570 V, between the electrode pin pairs. Patches, soaked with 4 kDa fluorescein-isothiocyanate labeled dextran (FD), doxorubicin (DOX) or fentanyl (FEN), were applied to the skin before and after EP. The new monitoring system was developed based on the delivery of FD to and through the skin. FD relative quantity was determined with fluorescence microscopy imaging, in the treated region of the skin for topical delivery and in a segment of the mouse tail for transdermal delivery. The application of electric pulses for FD delivery resulted in enhanced transdermal delivery. Depending on the amplitude of electric pulses, it increased up to the amplitude of 360 V, and decreased at higher amplitudes (460 and 570 V). Topical delivery steadily enhanced with increasing the amplitude of the delivered electric pulses, being even higher than after tape stripping used as a positive control. The non-invasive monitoring of the delivery of DOX, a fluorescent chemotherapeutic drug, qualitatively and quantitatively confirmed the effects of EP at 360 and 570 V pulse amplitudes on topical and transdermal drug delivery. Delivery of FEN at 360 and 570 V pulse amplitudes verified the observed effects as obtained with FD and DOX, by the measured physiological responses of the mice as well as FEN plasma concentration. This study demonstrates that with the newly developed non-invasive multi-array electrodes and with the varying electric pulse amplitude, the amount of topical and transdermal drug delivery to the skin can be controlled. Furthermore, the newly developed monitoring system provides a tool for rapid real-time determination of both, transdermal and topical delivery, when the delivered molecule is fluorescent.

1. Introduction

Transdermal drug delivery offers an attractive non-invasive alternative to the conventional delivery methods, such as oral administration and injection. The main advantage of the delivery through skin is the possibility of molecules to enter the circulation, avoiding the metabolic processing of the delivered molecules in the liver. However, the stratum corneum acts as a limiting barrier, therefore only small lipophilic drugs have the ability to penetrate the skin at therapeutic rates by passive diffusion [1,2]. Conventional transdermal delivery systems, such as transdermal patches, enable controlled transdermal drug delivery, but are applicable only to small, potent and lipophilic solutes and the transport of drug across the skin is slow with lag times to reach steady-state fluxes in hours [2,3]. Therefore, to deliver larger molecules with therapeutic drug levels, many chemical and physical delivery methods were developed [4]. Many studies were focused on so-called active strategies such as sonophoresis [5–9], iontophoresis [10–12] and electroporation [1,13–17]. However, the existing monitoring systems lack the real-time monitoring of topical and transdermal drug delivery, as well as the ability of its quantification.

Electroporation (EP) is a physical method for the delivery of molecules into the cells and tissues [18,19]. Currently its biomedical applications are the delivery of (i) chemotherapeutics (electrochemotherapy) [20,21], (ii) naked plasmid DNA or RNA (gene electrotransfer) for tumor treatment and DNA vaccine [15,22–24] or (iii) drugs/DNA delivery in or across the skin [25–31]. EP mediated delivery of drugs and DNA

* Corresponding author at: Institute of Oncology Ljubljana, Department of Experimental Oncology, Zaloska 2, SI-1000 Ljubljana, Slovenia. Tel./fax: +386 15879434.
E-mail address: gsersa@onko-i.si (G. Sersa).

0168-3659/$ – see front matter © 2013 Elsevier B.V. All rights reserved.
http://dx.doi.org/10.1016/j.jconrel.2013.09.030

to the skin has already been successfully performed in rodent, porcine and non-human primate skin models [16,29,32,33]. For the delivery to the skin several different electrode types were used, from plate, needle, needle free microelectrode array to multi-electrode array [13,34–39]. Depending on the molecules to be delivered, long (ms) pulses are needed for naked DNA delivery, while short (μs) pulses can be used for the smaller molecules like drugs. Depending on the electrode type, the delivery of molecules can be controlled by the number, amplitude, and duration of electric pulses [13,40–42]. Non-invasive electrodes are particularly interesting to localize the electrical field in the skin [16]. However, EP using non-invasive multi-array electrodes with spring loaded pins was not tested yet for the controlled transdermal and topical drug delivery.

Besides the delivery of molecules to target cells in tissues, the application of electric pulses also has vascular effects on normal and tumor blood vessels [43–46]. On the experimental tumors it was shown that the vascular effects of EP, *i.e.* vasoconstriction and increased permeability of blood vessels, are dependent on the number and especially the amplitude of electric pulses. Namely, the vascular effects were observed only after certain threshold amplitude was reached and its further increase prolonged them [47]. Recently it was shown that EP can indeed increase the permeability of tumor blood vessels and with the use of intravital microscopy it was also confirmed on normal blood vessels in skin [44], meaning that EP induces vasoconstriction of all exposed blood vessels as well as increases their permeability [46,48]. Therefore, when EP is used for the topical and transdermal drug delivery, the vascular effects of EP should be taken into account.

In this study we investigated the relationship between the transdermal and topical drug delivery, controlled by EP of the skin. For this purpose we used a new non-invasive multi-array electrodes and different high-voltage EP parameters. In order to monitor the topical and transdermal delivery we developed a real-time monitoring system, based on fluorescently labeled molecules, that can qualitatively and quantitatively follow the extent of topical and transdermal delivery. Additionally, the established monitoring system was, as a proof of principle, also used for the topical and transdermal doxorubicin delivery. In order to verify the effect of pulse amplitude on transdermal and topical delivery as well as to verify the monitoring system, standard fentanyl assays [49] were also performed.

2. Materials and methods

2.1. Reagents and drugs

The 4 kDa fluorescein-isothyocianate (FITC) labeled dextran (FD) (Sigma-Aldrich, St. Louis, MO, USA) was resuspended in phosphate buffered saline (PBS). In order, to remove any free FITC or low-molecular weight contaminants, the FD was washed two times for 2 h through 2 kDa ultrafiltration spin column (Vivaspin, Sartorius Stedim Biotech, Goettingen, Germany). The component with high molecular weight was afterwards resuspended in PBS to a final concentration of 37.5 mg/mL. In addition, Doxorubicin hydrochloride (DOX) obtained from Teva (Teva Pharmaceutical Industries Ltd, Pharmachemie B.W., Haarlem, Netherlands) and Fentanyl (FEN) purchased from Chiesi PharmaceuticalGmbH (Torrex; Chiesi Pharmaceutical GmbH, Wien, Austria) were used as model drugs to study the extent of transport into and through mouse skin into systemic circulation. The concentration of stock FD solution was 37.5 mg/mL [46,48] and concentration of stock FEN solution was 50 μg/mL. Epirubicin hydrochloride, which was used as an internal standard for chemical analysis, was purchased at Actavis (Episinidan; Actavis, Hafnarfjordur, Iceland). LC–MS grade acetonitrile and water used as mobile phases were purchased at J.T. Baker (Phillipsburg, NJ, USA), whereas the mobile phase additive formic acid (50%) was obtained from Sigma-Aldrich. All solvents and chemicals employed in sample preparation (methanol, water and sodium acetate) were of analytical grade purity.

2.2. Animals and skin preparation

In the experiments 10–12-week old female BALB/c mice (Harlan Laboratories, Udine, Italy) weighing between 20 to 25 g were used. Mice were kept under specific pathogen-free condition at a constant room temperature and humidity and at 12 h light/dark cycle. Food and water were provided *ad libitum*. All experiments were conducted in accordance with the guidelines for animal experiments of the EU directive and permission from the Ministry of Agriculture and the Environment of the Republic of Slovenia (permission 34401-1/2012/4). For each experimental condition 3–6 mice were randomly assigned. Mice were shaved on the flank region and any remaining hair was removed with depilatory cream (Vitaskin; Krka, Novo mesto, Slovenia). Moreover, to reduce the autofluorescence, the tail of mice was also depilated before the experiments with FD and DOX where fluorescence microscopy imaging was employed.

2.3. Drug application

In all experiments a circular patch with the diameter of ~1 cm (Tosama d.o.o., Domzale, Slovenia) served as a reservoir for molecules or drug application. In case of EP the patch soaked with FD (110 μL of 37.5 mg/mL), DOX (100 μL in dose of 10 mg/kg) or FEN (~120 μL in dose of 0.3 mg/kg) was applied on the depilated mouse flank region for 5 min, which was first rinsed with a piece of wet cotton. The patch was removed during the EP and afterwards it was reapplied and left on the skin for 1 h. Subcutaneous injection of the equal quantity of FD, DOX or FEN, as applied on the patches, was referred as 100% transdermal delivery. The tape stripping method [50] served as a positive control. An adhesive tape-strip was placed and gently pressured onto the depilated area of mouse skin, by which a good contact with skin was ensured. Subsequently, the tape was removed with sharp upward movement. These two steps were repeated 15–20 times, which enabled the removal of the stratum corneum layer.

2.4. Electrodes and EP parameters

The non-invasive multi-array electrodes, consisting of 7 spring loaded pins arranged on hexagonal mesh and spaced 3.5 mm between each other, were provided by Iskra Medical (Podnart, Slovenia) (specifics are provided in the Supplementary material and methods). Electrodes were connected to the CLINIPORATOR™ (IGEA s.r.l., Carpi, Italy). Different short high voltage square wave pulses (amplitude between 70 and 570 V) with duration of 100 μs were used for the transdermal delivery of FD. A total of 24 electric pulses (2 electric pulses between each electrode pair) were delivered during the treatment. For transdermal delivery of DOX and FEN only the amplitudes 360 V and 570 V were applied.

2.5. Fluorescence microscopy and image acquisition

Fluorescence microscopy was carried out with a Zeiss SteREO Lumar.V12 (Zeiss, Jena, Germany) fluorescence stereomicroscope equipped with an MRc.5 digital camera (Zeiss). Animals were initially anesthetized with inhalation anesthesia in the induction chamber (Isofluoran; Nicholas Piramal India, London, UK) and placed under the microscope, with their snout in the inhalation tube to remain anesthetized during the experiment. Furthermore, the tail was fixed with adhesive tape (Micropore, 3M Health Care, Neuss, Germany) on each side outside the field of view of the microscope to prevent its movement during the observation. To obtain 48-bit RGB images of emitted fluorescence light the appropriate filters (FD (excitation: 470/40 nm; emission: 525/50 nm), DOX (excitation: 470/40 nm; emission: LP 515 nm)) were used. A time series of images were acquired with the following timeline; firstly, one image was acquired before the application of the patch and another 5 min later, when the patch was removed for EP; afterwards,

an image was acquired immediately after EP and every 5 min for 1 h. Furthermore, after removal of the patch, the images of electroporated region of the skin were acquired. The first image was taken 1 h post-treatment and the rest of them followed at 2, 3, 4, 7, 24 and 48 h post-treatment. The files were stored and analyzed off-line with image analysis software AxioVision (Zeiss). Further details of experimental procedure are given in Supplementary materials and methods.

2.6. Image and data analysis

The increase in fluorescence intensity in the tail and in the area of the electroporated skin was determined by means of AxioVision (Zeiss). To determine the increase of fluorescence intensity in the tail, the images were combined into a logical time series and then a binary mask of the fluorescent part of the tail in every time point was created by applying a suitable threshold, which was kept constant for the entire time series. Subsequently the mean fluorescence intensity within the masked region was determined on the original images. The increase of fluorescence intensity was normalized to the value determined on the image acquired 5 min post-treatment (when linear increase of FD fluorescence intensity in the tail region was achieved) and expressed as a percentage of the fluorescence intensity increase of the subcutaneous injection at the same time point. To determine the extent of topical delivery of molecules, the acquired images of the electroporated region of the skin were analyzed. Similar to the above described analysis, the images were combined in a logical time series and then a threshold was determined on every image to create a binary mask of the area exhibiting increased fluorescence intensity in comparison to the non-electroporated skin. These binary masks were used to measure the area of the successful topical delivery and the mean fluorescence intensity within this area. The data was then normalized to the first acquired image at 1 h post-treatment and expressed as a percentage of fluorescent area or fluorescence intensity change.

2.7. Fentanyl delivery by EP

The pharmacodynamics of anesthetic FEN was performed as previously described [49]. Briefly, mice were tested for nociceptive response with the tail withdrawal assay (TWA) with slight modifications, where the tail was exposed to hot plate instead to hot water. Animals were placed in a cylindrical mice holders (Harvard Apparatus, Massachusetts, USA) with their tail hanging freely outside the holder. The distal 3 cm of the tail was exposed to a hot plate with 60 ± 0.5 °C and the time needed for tail withdrawal (latency) was measured to the nearest 0.01 s. In order to minimize the tissue damage and burns a cut-off time of 15 s was used. Furthermore, additional supraspinal side effects were evaluated, where the decrease of responsiveness, testing pinna, cornea and muscle reflexes, was determined by scoring the induced level of analgesia. Reflexes were scored as 0 (normal reflex), 1–2 (slightly or marked attenuated reflex) or 3 (absence of reflex) [49]. Measurements of all physiological responses (nociceptive response, cornea reflex, pinna reflex and muscle reflex) described above were performed before the application of the drug and then every 15 min for 5 h.

To select an appropriate dose of FEN for the experiments with EP the calibration curves of the assays were performed. Several doses of freshly prepared FEN solutions in 0.9% NaCl (0.01, 0.025, 0.05, 0.1, 0.2 and 0.3 mg/kg) or 0.9% NaCl alone were injected subcutaneously, to define the response of the mice at a certain dose of the drug. On the basis of the calibration curves (Supplementary Fig. S8) a dose of 0.3 mg/kg of FEN was selected for experiments with EP.

The results of cornea, pinna and muscle reflexes are presented as mean values of the determined score within the test. The determined latency with TWA was expressed as percentage of maximal possible effect (% MPE), which was calculated according to Eq. 1 [49]. To determine the efficiency of EP mediated transdermal delivery of FEN, the results obtained in the physiological response tests were normalized to the response induced by subcutaneous injection in the same test, and expressed as a % of the response of the subcutaneous injection in that test. Subsequently, these results were then pooled to give a single value representing the mean effect of the delivered FEN in all four tests in comparison to the subcutaneous injection.

$$\%\ MPE = \frac{post-treatment\ latency\ (s) - pre-treatment\ latency\ (s)}{cut-off\ time\ (15\ s) - pre-treatment\ latency\ (s)} \times 100 \quad (1)$$

2.8. Blood collection and plasma preparation

To confirm the transdermal delivery of DOX obtained by measurement of fluorescence in the tail region, the DOX concentration in plasma was determined 15 min post-treatment. Furthermore, FEN concentration in blood plasma was determined as well. Initially, in the calibration curve experiments with FEN, the blood was collected 15 or 60 min post-treatment and in the experiments with EP the blood was collected 15 min post-treatment.

Blood was collected from the mouse retro-orbital sinus, with a fine-walled glass Pasteur pipettes (BRAND GMBH + CO KG, Wertheim, Germany), containing anticoagulant sodium citrate (3.2%, 0.109 M, pH 7.4). Not more than 200 μL of blood per mouse was collected into a plastic tube containing sodium citrate in a ratio 9:1, from which the blood plasma was prepared by centrifugation for 10 min at $3000 \times g$ at room temperature. Afterwards, plasma was re-pipetted into fresh plastic tubes and stored at −20 °C until further analysis. Blood was taken only once from each animal.

2.8.1. Determination of FEN plasma levels by gas chromatography/mass spectroscopy (GC/MS)

Premeasured volumes of 30–100 μL plasma were diluted in 3 mL 100 mM sodium acetate and internal standard citalopram (10 ng/mL) was added. Samples were sonicated (30 min), vortexed and loaded on Strata X-CW 60 mg/3 mL cartridges (Phenomenex, CA, USA), which were preconditioned with 3 mL of acetone and methanol, deionized water and 100 mM sodium acetate. Subsequently, the sorbent was washed with 100 mM sodium acetate and acetic acid, and 50% methanol, dried and eluted with 2×0.6 mL triethylamine/methanol (5/95) and 0.6 mL triethylamine/acetone (5/95). The eluant was dried and reconstituted in 100 μL toluene. Gas chromatograph coupled to 240-MS (Agilent Technologies, CA, USA) was employed for GC–MS/MS analyses using DB-5 MS (Agilent Technologies) capillary column. The GC oven was programmed at 100 °C for 2 min, ramped at 20 °C/min to 300 °C, and held for 3 min. FEN eluted at 13.8 min and was quantitatively determined based on the transition 245→146. Limit of quantification (LOQ) was determined as the lowest calibration point where the coefficient of variability (CV) did not exceed 20% and was 1 ng/mL.

2.8.2. Determination of DOX plasma levels by liquid chromatography/mass spectroscopy (LC/MS)

Premeasured volumes of 50–100 μL plasma were diluted in 1 ml sodium acetate (100 mM) and internal standard epirubicin (250 ng/mL) was added. Samples were sonicated (30 min), vortexed and loaded on Oasis HLB 30 mg/mL cartridges (Waters Corp., MA, USA), which were preconditioned with 1 mL methanol, deionized water and 100 mM sodium acetate. After sample loading cartridges were dried and eluted with 3×0.6 mL of formic acid/methanol (2/98). The eluant was dried and reconstituted with 100 μL of 0.1% formic acid/acetonitrile (8/2). Quantitative analysis was performed using Waters Acquity ultra-performance liquid chromatograph (Waters Corp.) coupled to a Waters Premier quadrupole time-of-flight mass spectrometer. Separation was achieved at a flow rate of 0.3 mL/min by using Acquity UPLC™ BEH Shield C-18 ($1.7\ \mu m \times 2.1\ mm \times 50\ mm$, Waters Corp.) column with mobile phases 0.1% formic acid and acetonitrile. For doxorubicin and epirubicin their protonated molecules at 544.1819 ± 5 ppm were followed, at 1.19 min

and 1.31 min, respectively. The LOQ for DOX analytical method was 2 ng/mL with a predefined CV of less than 20%.

2.9. Histology

The region of the skin exposed to the treatment was excised at 1, 12, 24 and 48 h post-treatment. The excised skin was fixed in formalin for 24 h and then stored in 70% ethanol until embedding in paraffin. Subsequently, 5 μm thick sections were cut in the direction perpendicular to skin layers and stained with hematoxylin and eosin. To determine the depth of penetration of the molecules after different treatments, the treated region of the skin was excised 1 h post-treatment, immediately fixed in Zn fixative (BD Pharmingen™, BD Bioscience, San Diego, CA)) for 24 h and then stored in 70% ethanol until embedding in paraffin. Subsequently, 5 μm thick sections were cut. The prepared slides were observed with BX-51 microscope (Olympus, Hamburg, Germany) equipped with a digital camera DP72 (Olympus).

2.10. Statistical analysis

For statistical analysis Sigma Plot software (Systat software, London, UK) was used. Comparison between groups was done by using Student *t*-test or one-way analysis of variance (ANOVA) followed by a Holm–Sidak test. A value of $P < 0.05$ was considered statistically significant.

3. Results

3.1. In vivo real-time monitoring system: EP mediated transdermal and topical FD delivery

The developed system based on *in vivo* fluorescence imaging was used to evaluate the topical and transdermal drug delivery mediated by EP. EP of the dorsolateral mouse skin was performed with multi-array electrodes (Supplementary Fig. S1), which were firmly placed on the skin and 24 square wave electric pulses (2 between each electrode pair) of varying amplitudes (70–570) and duration 100 μs were delivered. Subcutaneous injection served as reference value for 100% transdermal delivery, while skin tape stripping was used as a positive control. The skin area where the delivery was performed was monitored by fluorescence stereo-microscope for the topical delivery whereas the segment of tail was monitored for the transdermal delivery. Fluorescence images that were captured were analyzed off-line for the fluorescence intensity and fluorescent area, which enabled quantification of the delivered FD (Fig. 1A, B). The system is extensively described in Supplementary materials and methods (Supplementary Figs. S2, S3).

Compared to the subcutaneous injection of FD, EP induced transdermal delivery of FD up to 16%. When the tape stripping method (positive control) was used, the achieved transdermal delivery was higher (23%), but there was no statistically significant difference compared to EP mediated delivery when electric pulses with the amplitude of 360 V were used. The transdermal FD delivery was controllable by electrical parameters of the pulses; namely with increasing the amplitude of the delivered pulses, a steady increase of transdermal FD delivery was determined up to 360 V where a peak of the transdermal delivery was observed. With further increase of the amplitude of the electric pulses, the extent of transdermal delivery decreased (Figs. 1A, 2A; Supplementary Fig. S4).

Topical delivery was determined even with the lowest amplitude of electric pulses, and steadily increased with increasing the amplitude up to 570 V (Fig. 1B). Compared to the tape stripping method (positive control), EP proved to be statistically significantly more effective at the highest amplitude at 48 h post-treatment. As demonstrated in Fig. 2 (B, C), with increasing the amplitude, the area of permeabilized region of the skin as well as fluorescence intensity (quantity of FD uptake into the cells) was increasing. The uptake process was fast with maximal

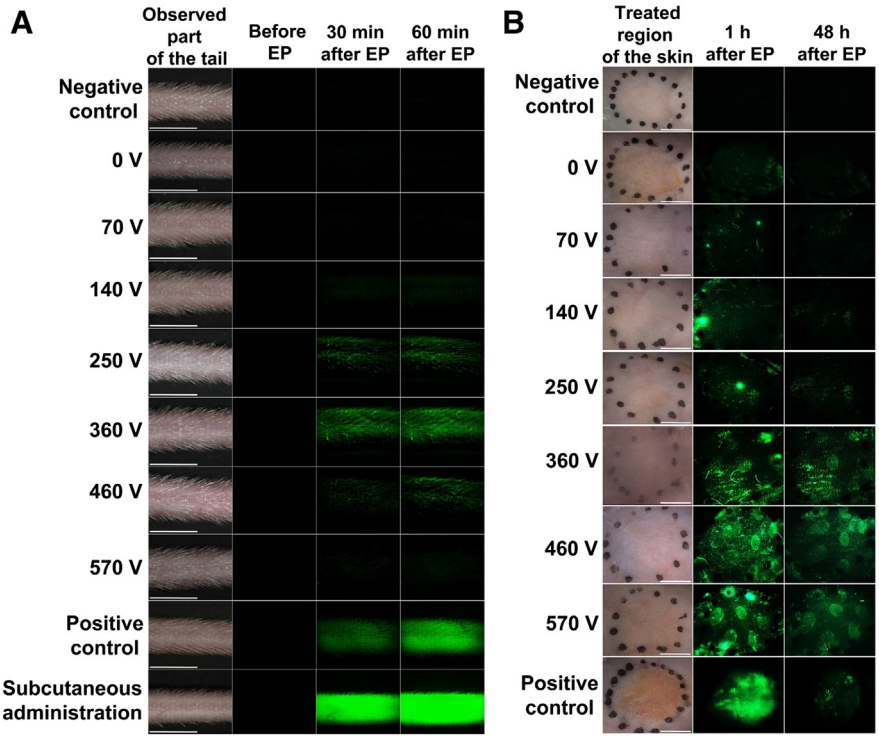

Fig. 1. Images of topical and transdermal FD delivery. (A) Representative images of the observed part of mice tails showing the increase of fluorescence intensity due to the transdermal delivery by EP on the flank of the mice, tape stripping method (positive control) or subcutaneous injection of FD. Images were acquired at designated times. Scale bar: 5 mm. (B) Representative images of the observed regions of the skin showing the successful topical delivery of FD by EP or tape stripping method (positive control) and its retention in the treated region of the skin. The predetermined area for the treatment was marked with permanent marker (black dotted marks). Images were taken at designated times. Scale bar: 5 mm. 0, 70, 140, 250, 360, 460, 570 V — EP with selected amplitude; negative control — non-treated group; positive control — removal of stratum corneum with tape stripping method. For graphical representation the images were processed with Fiji software [51].

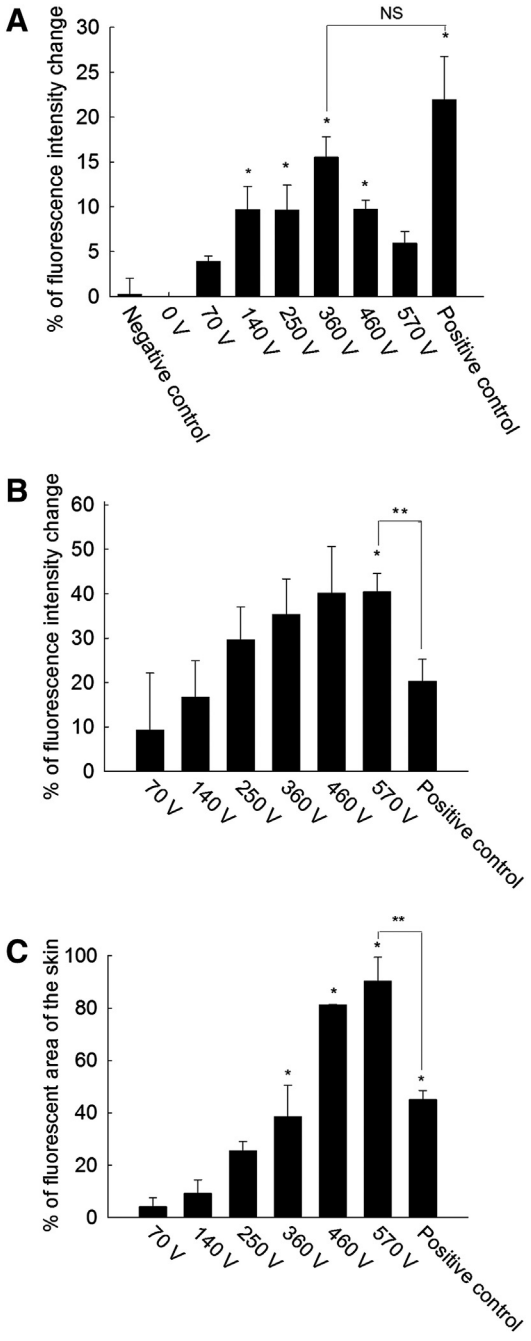

Fig. 2. Fluorescence intensity changes in the tails and in the skin of the mice after topical and transdermal delivery of FD mediated by EP. (A) Transdermal FD delivery — % of fluorescence intensity change 50 min after EP normalized to subcutaneous administration. Subcutaneous administration stands for a reference value 100% of transdermal delivery. (B) Topical FD delivery — fluorescence intensity change of topically delivered FD 48 h post-treatment and (C) change in the area of permeabilized region of the skin 48 h post-treatment, normalized to fluorescence intensity or permeabilized area 1 h after EP. 0, 70, 140, 250, 360, 460, 570 V — EP with selected amplitude; negative control — non-treated group; positive control — removal of stratum corneum with tape stripping method. n = 3–6 mice per group. * P value <0.05 *vs.* negative control, 0 V (transdermal delivery) and *vs.* 70 V (topical delivery), ** P value <0.05 between marked groups, NS = no statistical significant difference. Error bars indicate SEM.

elution of FD in the first hours, and afterwards the elution process slowed down during the 48 h observation time. The elution of FD in the first hours was probably due to the wash out from the extracellular matrix and the level of the remaining fluorescent area represents intracellular FD presence as an indicator of successful permeabilization of cells (Supplementary Fig. S5). As shown in Fig. 1B the delivery of FD to skin was evident particularly underneath the electrodes, indicating on higher cell permeabilization and FD uptake in the area underneath the electrode pins.

3.2. Doxorubicin delivery as proof of principle

EP, with two selected amplitudes (360 and 570 V), which were selected to verify the differences between the transdermal deliveries as observed with FD, was also used for transdermal and topical delivery of DOX monitored by monitoring system (Fig. 3A, B). The results correlated with FD and confirmed that the amount of transdermal DOX delivery was lower when delivery was mediated with the higher amplitude applied (570 V). Besides measuring the DOX fluorescence intensity in the observed tail region (Fig. 4A; Supplementary Fig. S6), the amount of DOX was also quantified in blood plasma (Fig. 4B; Supplementary Table S1). Topical delivery was again depended on the amplitude of electric pulse; higher amplitude provided larger permeabilized area and also higher quantity of DOX in the skin (Fig. 5, Supplementary Fig. S7). Besides the dotted fluorescent skin area underneath the electrode pins after EP (Fig. 3B), another evidence of EP mediated topical DOX delivery was also observed in the treated region of the skin, where DOX caused destruction of hair follicle cells leading to temporary alopecia (lasting ~4 days) (Fig. 6A). The damage to the skin was more pronounced with tape stripping method, since DOX was applied directly to the epidermis, due to the removed stratum corneum. Therefore, the formation of the crust was observed within 48 h (Fig. 6B). With subcutaneous injection of DOX minimal skin damage was observed only at the site of DOX injection (data not shown).

3.3. Verification of the model with fentanyl assays

In order to confirm the effect of pulse amplitude and to validate the *in vivo* non-invasive monitoring system, the FEN was also delivered by EP at two selected amplitudes – 360 and 570 V. The FEN analgesic activity measured by measuring cornea reflex, pinna reflex, muscle reflex, tail withdrawal latency and FEN plasma levels was less pronounced at the electric pulses with the amplitude of 570 V than at 360 V (Supplementary Fig. S9). Furthermore, the degree of physiological responses between the EP, subcutaneous injection and tape stripping method (positive control) was in the same relationship as demonstrated with the FD and DOX, monitored by monitoring system (Fig. 7A). The data were confirmed by the quantitative measurements of FEN in the blood plasma (Fig. 7B). Analgesic responses data and the FEN plasma concentration including the data obtained in the FEN calibration curves experiments are provided in Supplementary information (Supplementary Figs. S8, S9; Supplementary Tables S2, S3).

3.4. Histological evaluation of the skin after EP

Possible skin damage due to the application of EP was evaluated in the exposed region of the skin at 1, 12, 24, and 48 h post-treatment (Fig. 8A). Macroscopically, no skin damage was observed; neither skin burns, erythema or edema. Furthermore, microscopically hair follicles damage or severe damage of vasculature was not observed. Though, small presence of edema was observed at 1 and 12 h after EP with amplitudes of electric pulses of 360 and 570 V. Parakeratosis was also observed at these time point and 24 h post-treatment. Hyperplasia of epidermis was visible at 24 and 48 h post-treatment with EP at both amplitudes, but was more pronounced at the higher amplitude. According to the size of the skin damage, we assume that the damage was underneath the placed electrodes (Fig. 8B).

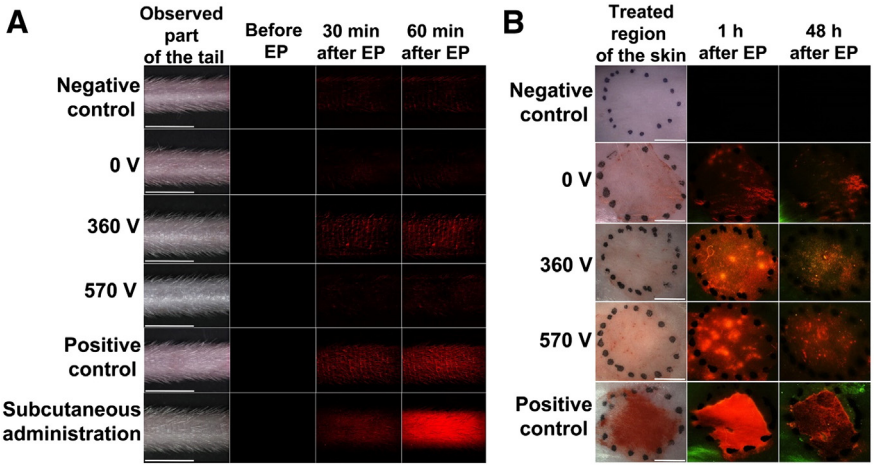

Fig. 3. Images of topical and transdermal DOX delivery. (A) Representative images of the observed part of mice tails showing the increase of fluorescence intensity due to the transdermal delivery by EP on the flank of the mice, tape stripping method (positive control) or subcutaneous injection of DOX. Images were acquired at designated times. Scale bar: 5 mm. (B) Representative images of the observed regions of the skin showing the successful topical delivery of DOX by EP or tape stripping method (positive control) and its retention in the treated region of the skin. The predetermined area for the treatment was marked with permanent marker (black dotted marks). Images were taken at designated times. Scale bar: 5 mm. 0, 360, 570 V — EP with selected amplitude; negative control — non-treated group; positive control – removal of stratum corneum with tape stripping method. For graphical representation the images were processed with Fiji software [51].

3.5. Histology; depth of penetration

One hour post-treatment the skin treated with DOX or FD was excised, embedded in paraffin and skin slides without staining were prepared. By imaging the fluorescence of the skin, penetration of the experimental molecule in and through the skin, mediated by electric pulse application or molecule alone, was evaluated. The DOX and FD penetration through skin was observed after removing the stratum corneum with tape stripping method, where FD and DOX penetrated through the skin. The penetration of FD and DOX was also observed after EP with both amplitudes, 360 and 570 V, but was less pronounced than after removal of stratum corneum (Fig 9).

4. Discussion

In this study we demonstrate that transdermal and topical drug delivery can be controlled by varying the amplitude of the electric pulses applied *via* novel multi-array spring loaded pin electrodes. Furthermore, we present a newly developed *in vivo* non-invasive monitoring system to visualize and quantitate transdermal and topical drug delivery, based on measurements of fluorescence intensity. Using different molecules to study transdermal delivery, we show the feasibility of our monitoring system. In addition, the suitability for monitoring topical delivery was also confirmed by imaging of DOX, a fluorescent chemotherapeutic molecule.

Several studies have dealt with the EP mediated delivery of different molecules to skin, using plate electrodes, invasive needle electrodes, non-invasive needle-free electrodes, needle free microelectrode or multi-electrode array [13,16,35–39,52]. The design of the electrodes, *i.e.* their tips in the case of needle electrodes varies substantially, however this is also reflected on the efficiency of delivery and also on the degree of the skin damage. It was demonstrated that by application of appropriate electric pulses, molecules such as fentanyl, insulin, methotrexate, calcein and fluorescently labeled dextrans, can be delivered transdermally, mostly quantified by blood analysis, and topically, by employing different microscopy techniques and skin sample chemical analysis [36,38,41,53–56]. Besides for drugs, EP following intradermal injection was shown to be effective also for plasmid DNA delivery into the skin cells, for the purpose of vaccination or therapeutic effects, aimed at various diseases, especially for cancer treatment, wound healing, ischemia and protein deficiency disorders [57–60]. For all these purposes, the advantage would be the use of non-invasive electrodes, by which the delivery of electric pulses does not damage the skin but can successfully permeabilize the stratum corneum, and also permeabilize the cells in epidermis to deliver the desired molecules into them. Such electrodes, the multi-electrode array (MEA), were designed by Heller et al. and have proved to be suitable for the delivery of plasmid DNA to skin when an intradermal injection of plasmid DNA was combined with EP [16,61–63]. With the application of several ms long, high voltage pulses they demonstrated the transfection of cells in the skin. In addition, electrodes with two parallel rows of four 2-mm pins and 4×4 minimally invasive electrode array were also designed and proved to be suitable for plasmid DNA delivery into the skin [64,65]. Our electrodes with similar design, with a larger gap between the pins, could probably be used also for plasmid DNA delivery to skin, however this topic was beyond the scope of this paper. In our study, we used these non-invasive multi-array electrodes with short (μs) high voltage electric pulses for delivery of different small molecules. We demonstrated that they can be delivered topically as well as transdermally. As evident from the images of the skin treated with fluorescent molecules (FD, DOX), the delivery was restricted to the area of the skin in contact with the electrodes. Specifically, with the increasing amplitudes of electric pulses the area of the skin where the fluorescent molecules were detected increased. However, controlled delivery of the molecules, as in our case FD, DOX and FEN, can be obtained by varying the amplitude of the electric pulses, without skin damage.

Usually skin diseases, such as psoriasis, contact dermatitis and skin cancer, require treatment which will ensure the delivery of drugs into the target cells. Our results demonstrate that the use of high voltage, μs pulses and multi-array electrodes where two pulses are delivered between each electrode pair (24 electric pulses in total), resulted in the delivery of drugs into the skin. The topical drug delivery was prolonged and visible for at least 48 h. Furthermore, with increasing the amplitude of delivered electric pulses, we could demonstrate the increase in the area of the permeabilized skin, as well as the increased uptake of molecules. Besides topical also transdermal delivery of molecules was demonstrated. The measurements of the systemically delivered molecules showed that transdermal delivery parallels the topical delivery up to the amplitude of electric pulses of 360 V. The transdermal delivery was presumably due to the intravasation of the molecules into the blood vessels, facilitated by effects of the electric pulses on the endothelial cells. In our previous studies we have demonstrated the vascular

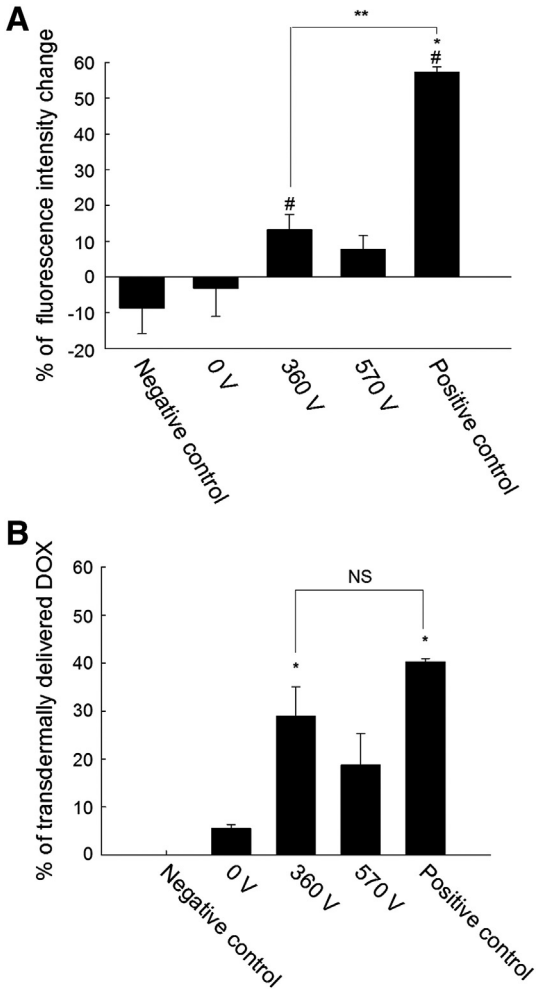

Fig. 4. Fluorescence intensity changes in the tails of mice and the quantity of DOX in the blood plasma after topical and transdermal delivery of DOX mediated by EP. (A) Transdermal DOX delivery — % of fluorescence intensity change 50 min after EP normalized to subcutaneous administration. Subcutaneous administration stands for a reference value 100% of transdermal delivery. (B) Quantity of DOX in blood plasma collected 15 min post-treatment expressed as a % of the quantity of DOX in the blood plasma after its subcutaneous injection. 0, 360, 570 V — EP with selected amplitude; negative control — non-treated group; positive control — removal of stratum corneum with tape stripping method. n = 3–6 mice per group. * P value <0.05 *vs.* negative control and 0 V, ** P value <0.05 between marked groups, NS = no statistical significant difference; # P value <0.05 (*t*-test) *vs.* negative control. Error bars indicate SEM.

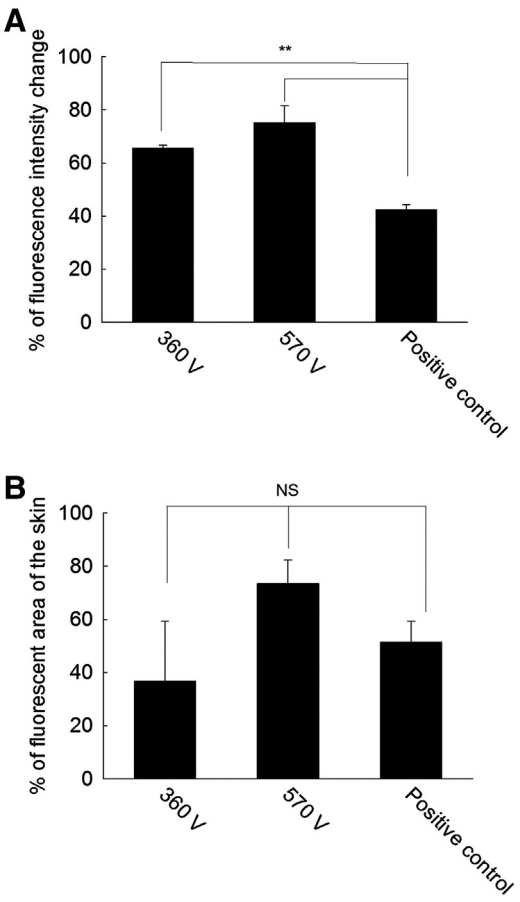

Fig. 5. Topical delivery of DOX. (A) The fluorescence intensity change 48 h post-treatment and (B) change in fluorescent area of permeabilized skin 48 h post-treatment. All data were normalized to the value 1 h after EP. 0, 360, 570 V — EP with selected amplitude; negative control — non-treated group; positive control — removal of stratum corneum with tape stripping method. n = 3–6 mice per group. ** P value <0.05 between marked groups, NS = no statistical significant difference. Error bars indicate SEM.

effects of EP, inducing increased permeability of the endothelial lining *in vitro* and *in vivo* and the extravasation of molecules in micro-vessels *in vivo* [46,48,66]. By these effects, also in the normal vessels in subcutis, the endothelial lining would be permeable and prone for intravasation of molecules. Furthermore, we have demonstrated that the vascular effects are threshold dependent and are also dependent on the amplitude of electric pulses, namely in tumors we have demonstrated that with low amplitudes of electric pulses the blood flow was increased and with the higher ones it was reduced or stopped [47]. Therefore, when the amplitude of electric pulses exceeds certain level, as in this study 360 V, the vasoconstricting effects of electric pulses would increase as well as the vessels permeability and consequently perfusion delay would be prolonged. Likewise, with increasing the pulse amplitude, the cell permeability and cellular drug uptake would be increased. Considering all mentioned effects of high voltage pulses the transdermal drug delivery would be hampered. The study thus demonstrates that with varying the amplitude of electric pulses we can control the topical and transdermal delivery of molecules, as shown with FD, DOX and FEN.

The mouse skin is not an ideal model to study topical and transdermal drug delivery. However it provides a good starting model that can be elaborated on pig and human skin models [67]. In our study we developed fluorescence based monitoring system that provides *in vivo* in real time, qualitative and quantitative information about topical and transdermal drug delivery. The system was developed with FD, which was applied on the skin before and after the application of electric pulses. The images of the trapped FD in the treated region of the skin were taken, from which the fluorescent area was measured, providing evidence for skin permeabilization, particularly underneath the electrode pins. The intensity of the fluorescence was the measure of the quantity of the molecules delivered topically to the skin. Furthermore, imaging the fluorescence intensity of a segment of the mouse tail provided indication on the quantity of the circulating FD and also provided information of the quantity of the molecule delivered transdermally in comparison to the positive control – the tape stripping method and subcutaneous injection of the molecules. Such non-invasive real-time method, for qualitative and quantitative monitoring of topical and transdermal drug delivery, has not been described yet. By using this monitoring system, EP proved to be effective also for the skin delivery of DOX, a fluorescent cytotoxic drug used in cancer treatment. We used two amplitudes (360 V and 570 V) that have proved to differ in the quantity of transdermally delivered FD. The demonstrated difference of quantified DOX by monitoring system as well as by biochemical quantification in the blood plasma corroborated the observation with FD. In addition, to verify new monitoring system, we compared the

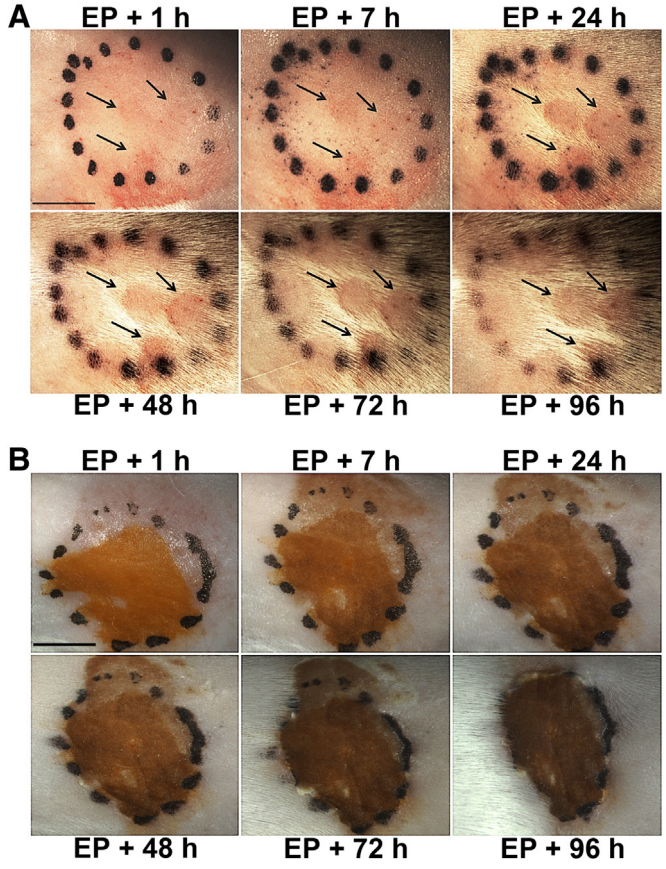

Fig. 6. Alopecia induced by DOX delivery. (A) Alopecia temporarily induced with the topical DOX delivery mediated by EP with amplitude of 570 V. DOX was topically delivered with EP and then images were acquired at designated times. Arrows mark the position of electrodes and subsequent development of alopecia underneath the electrodes. Regrowth of hair is observed 96 h after EP. (B) The damage to the skin with tape stripping method was substantial; leading to crust formation within 48 h. The predetermined area for the treatment was marked with permanent marker (black dotted marks). Scale bar: 5 mm.

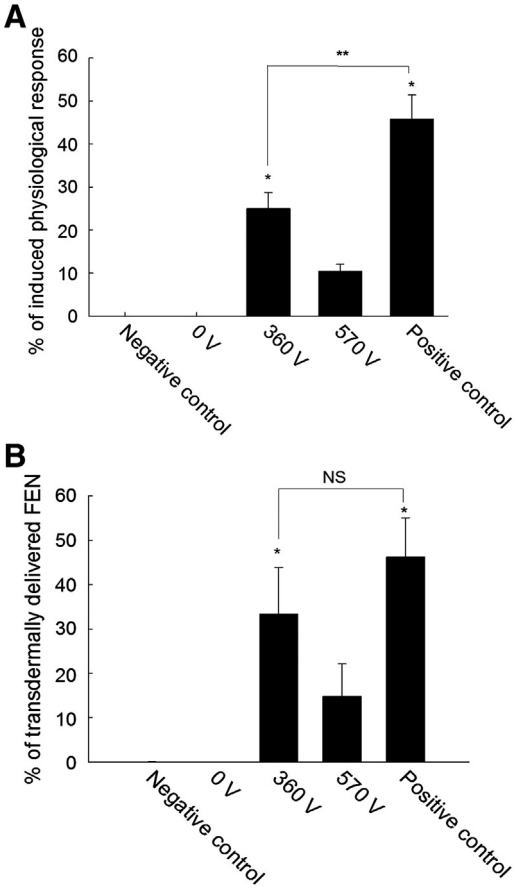

Fig. 7. Pharmacodynamics assays of FEN and quantity of FEN in the blood plasma after EP mediated transdermal delivery. (A) The determined physiological responses (cornea reflex, pinna reflex, muscle reflex, tail withdrawal latency) to FEN expressed as a % of the responses induced with the subcutaneous injection of FEN. (B) Quantity of FEN in blood plasma collected 15 min post-treatment expressed as a % of the quantity of FEN in the blood plasma after its subcutaneous injection. 0, 360, 570 V — EP with selected amplitude; negative control — non-treated group; positive control — removal of stratum corneum with tape stripping method. n = 3–6 mice per group. * P value <0.05 *vs.* negative control and 0 V, ** P value <0.05 between marked groups, NS = no statistical significant difference. Error bars indicate SEM.

results obtained with FD and DOX, by performing already established fentanyl assays, where physiological responses of mice to FEN are measured. The results with FEN delivery by EP at 360 and 570 V amplitudes matched those with FD and DOX and were further supported by biochemical quantification of FEN in the blood plasma of mice.

The use of novel non-invasive multi-array electrodes as used in our study was demonstrated to be minimally damaging, without skin burns, edema or erythema, with only microscopically visible parakeratosis and hyperplasia. Similar observation, but observed on macroscopic level, was also demonstrated by Heller's group with MEA, where longer electric pulses were used [35]. This study also reports on the occurrence of ulceration and necrosis after EP. Some studies resulted in severe skin damage, after application of low voltage electric pulses, such as redness of the skin, burnings, scars and skin lesions [63,68,69]. Therefore, for drug or gene electrotransfer to skin, the amplitude and duration of electric pulses are important. However, in order to minimize the pain the amplitude should be as low as possible; that can be obtained by reducing the distance between the electrode pins as much as possible. In our study, the tested electric pulse amplitudes have not caused skin damage, but were effective for topical and transdermal drug delivery in the range of molecules up to 4 kDa. The effectiveness of DOX delivery to the skin has also been demonstrated by the skin damage of the treated areas where temporary alopecia underneath the electrode surface was induced. The use of this delivery system might be effective also for the delivery of other larger molecules, such as plasmid DNA, with longer electric pulses and the cut-off size and yet to be determined.

5. Conclusion

In conclusion, our study provides first *in vivo* non-invasive fluorescence based monitoring system which is suitable for the determination of transdermal and topical delivery with qualitative and quantitative support. The transdermal and topical delivery depends on the amplitude of electric pulses applied and this can be a prominent variable in controlling drug delivery through skin. We are the first to describe and use non-invasive multi-array electrodes with spring loaded pins for the controlled topical and transdermal drug delivery to and through the skin.

Acknowledgments

This study was financially supported by Competency Center for Biomedical Engineering (CC BME) and was conducted within the scope of the EBAM European Associated Laboratory (LEA). This work is a result of networking efforts within COST TD1104 Action (www.electroporation.net). We would like to thank Iskra Medical d.o.o. for the providing of multi-array electrodes with spring loaded pins. We would like to thank Prof. Andrej Coer (Faculty of Health Sciences, University of Primorska, Slovenia) for his valuable comments in the evaluation of histological specimen. We would also like to thank Dr. Matej Rebersek, Barbara Zorec (University of Ljubljana, Faculty of

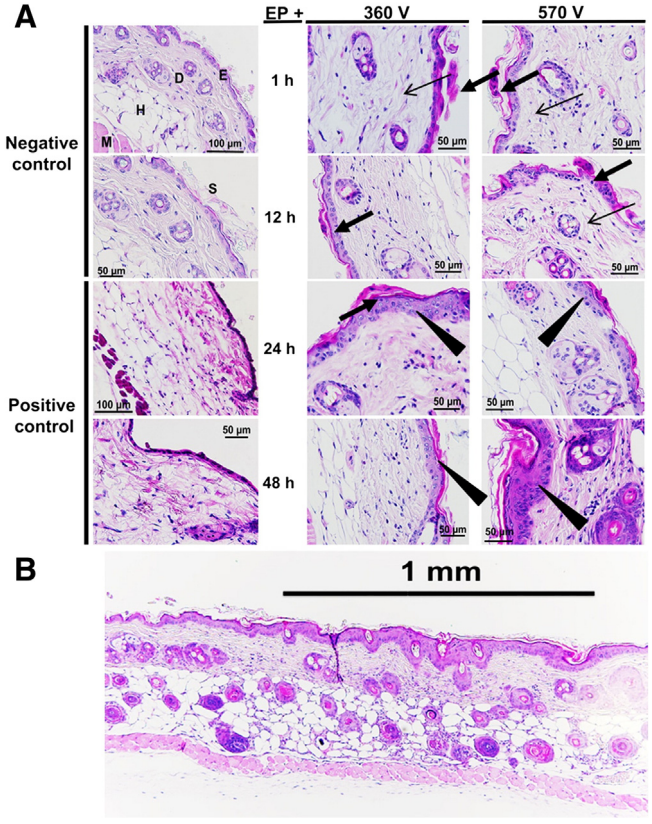

Fig. 8. Skin damage induced by EP after 1, 12, 24 and 48 h. Hematoxylin and eosin stained section of skin excised at indicated times after EP. (A) Negative control (E = epidermis; D = dermis; H = hypodermis; M = muscle; S = stratum corneum); in 1 h after EP edema (thin arrow) and parakeratosis (thick arrow) occurred. Hyperplasia (arrowhead) occurred after 24 and 48 h when skin was exposed to both tested amplitudes — 360 and 570 V pulses. (B) At 48 h post-treatment skin damage was observed only underneath the electrode surface. Scale bar indicates the position as well as the diameter of the electrode pin (2r = 1.3 mm).

Electrical Engineering, Slovenia), and Maja Ota (Institute of Oncology Ljubljana, Slovenia) for their technical support and all the work they contributed to this research.

Appendix A. Supplementary data

Supplementary data to this article can be found online at http://dx.doi.org/10.1016/j.jconrel.2013.09.030.

References

[1] M.R. Prausnitz, A practical assessment of transdermal drug delivery by skin electroporation, Adv. Drug Delivery Rev. 35 (1999) 61–76.
[2] J.J. Escobar-Chavez, D. Bonilla-Martinez, M.A. Villegas-Gonzalez, A.L. Revilla-Vazquez, Electroporation as an efficient physical enhancer for skin drug delivery, J. Clin. Pharmacol. 49 (2009) 1262–1283.
[3] R. Vanbever, V.V. Preat, *In vivo* efficacy and safety of skin electroporation, Adv. Drug Delivery Rev. 35 (1999) 77–88.
[4] B. Zorec, V. Preat, D. Miklavcic, N. Pavselj, Active enhancement methods for intra- and transdermal drug delivery: a review, Zdr. Vestn. 82 (2013) 339–356.
[5] B.E. Polat, P.L. Figueroa, D. Blankschtein, R. Langer, Transport pathways and enhancement mechanisms within localized and non-localized transport regions in skin treated with low-frequency sonophoresis and sodium lauryl sulfate, J. Pharm. Sci. 100 (2011) 512–529.
[6] B.E. Polat, W.M. Deen, R. Langer, D. Blankschtein, A physical mechanism to explain the delivery of chemical penetration enhancers into skin during transdermal sonophoresis — Insight into the observed synergism, J. Control. Release 158 (2012) 250–260.
[7] E.J. Park, J. Werner, N.B. Smith, Ultrasound mediated transdermal insulin delivery in pigs using a lightweight transducer, Pharm. Res. 24 (2007) 1396–1401.
[8] N.B. Smith, S. Lee, K.K. Shung, Ultrasound-mediated transdermal *in vivo* transport of insulin with low-profile cymbal arrays, Ultrasound Med. Biol. 29 (2003) 1205–1210.
[9] S. Mitragotri, J. Kost, Transdermal delivery of heparin and low-molecular weight heparin using low-frequency ultrasound, Pharm. Res. 18 (2001) 1151–1156.
[10] O. Pillai, R. Panchagnula, Transdermal delivery of insulin from poloxamer gel: *ex vivo* and *in vivo* skin permeation studies in rat using iontophoresis and chemical enhancers, J. Control. Release 89 (2003) 127–140.
[11] Y. Wang, R. Thakur, Q. Fan, B. Michniak, Transdermal iontophoresis: combination strategies to improve transdermal iontophoretic drug delivery, Eur. J. Pharm. Biopharm. 60 (2005) 179–191.
[12] H. Chen, H. Zhu, J. Zheng, D. Mou, J. Wan, J. Zhang, T. Shi, Y. Zhao, H. Xu, X. Yang, Iontophoresis-driven penetration of nanovesicles through microneedle-induced skin microchannels for enhancing transdermal delivery of insulin, J. Control. Release 139 (2009) 63–72.
[13] A.R. Denet, R. Vanbever, V. Preat, Skin electroporation for transdermal and topical delivery, Adv. Drug Delivery Rev. 56 (2004) 659–674.
[14] J. Gehl, Electroporation: theory and methods, perspectives for drug delivery, gene therapy and research, Acta Physiol. Scand. 177 (2003) 437–447.
[15] L.C. Heller, R. Heller, *In vivo* electroporation for gene therapy, Hum. Gene Ther. 17 (2006) 890–897.
[16] R. Heller, Y. Cruz, L.C. Heller, R.A. Gilbert, M.J. Jaroszeski, Electrically mediated delivery of plasmid DNA to the skin, using a multielectrode array, Hum. Gene Ther. 21 (2010) 357–362.
[17] V. Regnier, A. Tahiri, N. Andre, M. Lemaitre, T. Le Doan, V. Preat, Electroporation-mediated delivery of 3′-protected phosphodiester oligodeoxynucleotides to the skin, J. Control. Release 67 (2000) 337–346.
[18] T. Kotnik, P. Kramar, G. Pucihar, D. Miklavcic, M. Tarek, Cell membrane electroporation–Part 1: the phenomenon, IEEE Electr. Insul. Mag. 28 (2012) 14–23.
[19] S. Haberl, D. Miklavcic, G. Sersa, W. Frey, B. Rubinsky, Cell membrane electroporation–Part 2: the applications, IEEE Electr. Insul. Mag. 29 (2013) 29–37.
[20] D. Miklavcic, G. Sersa, E. Brecelj, J. Gehl, D. Soden, G. Bianchi, P. Ruggieri, C.R. Rossi, L.G. Campana, T. Jarm, Electrochemotherapy: technological advancements for efficient electroporation-based treatment of internal tumors, Med. Biol. Eng. Comput. 50 (2012) 1213–1225.
[21] G. Sersa, D. Miklavcic, M. Cemazar, Z. Rudolf, G. Pucihar, M. Snoj, Electrochemotherapy in treatment of tumours, Eur. J. Surg. Oncol. 34 (2008) 232–240.
[22] M. Cemazar, T. Jarm, G. Sersa, Cancer electrogene therapy with interleukin-12, Curr. Gene. Ther. 10 (2010) 300–311.
[23] J.M. Escoffre, J. Teissie, M.P. Rols, Gene transfer: how can the biological barriers be overcome? J. Membr. Biol. 236 (2010) 61–74.

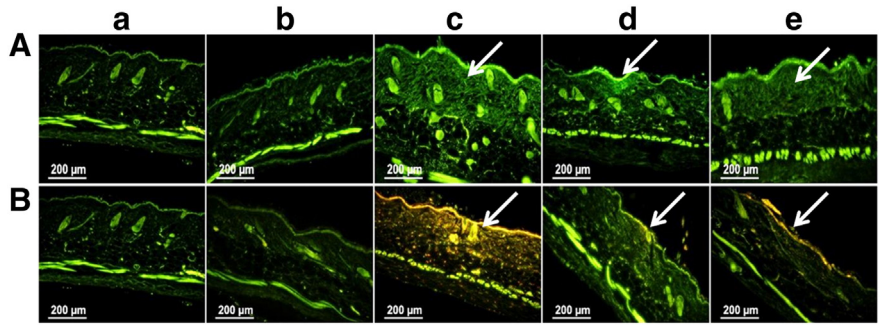

Fig 9. Depth of penetration of fluorescent molecules into the skin after EP. Penetration of (A) FD and (B) DOX 1 h post-treatment. Skin was excised 1 h post-treatment, fixed, embedded in paraffin and cut in orientation perpendicular to the skin layers. 5 µm thick unstained skin slides were prepared for each skin sample: (a) negative control, (b) passive diffusion (0 V), (c) positive control (tape strip), (d) skin subjected to 360 V electric pulses and (e) skin subjected to 570 V electric pulses. In (A) the increase of green fluorescence and arrows mark the presence of FD and in (B) the orange/red color and arrows indicate on presence of DOX in the skin.

[24] M. Linnert, H.K. Iversen, J. Gehl, Multiple brain metastases — current management and perspectives for treatment with electrochemotherapy, Radiol. Oncol. 46 (2012) 271–278.
[25] A.M. Bodles-Brakhop, R. Heller, R. Draghia-Akli, Electroporation for the delivery of DNA-based vaccines and immunotherapeutics: current clinical developments, Mol. Ther. 17 (2009) 585–592.
[26] B.M. Medi, J. Singh, Delivery of DNA into skin *via* electroporation, Methods Mol. Biol. 423 (2008) 225–232.
[27] L.C. Heller, M.J. Jaroszeski, D. Coppola, R. Heller, Comparison of electrically mediated and liposome-complexed plasmid DNA delivery to the skin, Genet. Vaccines Ther. 6 (2008) 16.
[28] T.E. Vaughan, J.C. Weaver, Mechanism of transdermal drug delivery by electroporation, Methods Mol. Med. 37 (2000) 187–211.
[29] N. Pavselj, V. Preat, DNA electrotransfer into the skin using a combination of one high- and one low-voltage pulse, J. Control. Release 106 (2005) 407–415.
[30] S. Mazeres, D. Sel, M. Golzio, G. Pucihar, Y. Tamzali, D. Miklavcic, J. Teissie, Non invasive contact electrodes for *in vivo* localized cutaneous electropulsation and associated drug and nucleic acid delivery, J. Control. Release 134 (2009) 125–131.
[31] A. Gothelf, J. Gehl, Gene electrotransfer to skin; review of existing literature and clinical perspectives, Curr. Gene. Ther. 10 (2010) 287–299.
[32] R. Vanbever, D. Fouchard, A. Jadoul, N. De Morre, V. Preat, J.P. Marty, *In vivo* noninvasive evaluation of hairless rat skin after high-voltage pulse exposure, Skin Pharmacol. Appl. Skin Physiol. 11 (1998) 23–34.
[33] J. Glasspool-Malone, S. Somiari, J.J. Drabick, R.W. Malone, Efficient nonviral cutaneous transfection, Mol. Ther. 2 (2000) 140–146.
[34] R. Vanbever, V. Preat, Transdermal drug delivery by skin electroporation in the rat, Methods Mol. Med. 37 (2000) 457–471.
[35] A. Donate, D. Coppola, Y. Cruz, R. Heller, Evaluation of a novel non-penetrating electrode for use in DNA vaccination, PLoS One 6 (2011) e19181.
[36] T.W. Wong, C.H. Chen, C.C. Huang, C.D. Lin, S.W. Hui, Painless electroporation with a new needle-free microelectrode array to enhance transdermal drug delivery, J. Control. Release 110 (2006) 557–565.
[37] S. Henry, D.V. McAllister, M.G. Allen, M.R. Prausnitz, Microfabricated microneedles: a novel approach to transdermal drug delivery, J. Pharm. Sci. 88 (1999) 948.
[38] W. Martanto, S.P. Davis, N.R. Holiday, J. Wang, H.S. Gill, M.R. Prausnitz, Transdermal delivery of insulin using microneedles *in vivo*, Pharm. Res. 21 (2004) 947–952.
[39] L. Daugimont, N. Baron, G. Vandermeulen, N. Pavselj, D. Miklavcic, M.C. Jullien, G. Cabodevila, L.M. Mir, V. Preat, Hollow microneedle arrays for intradermal drug delivery and DNA electroporation, J. Membr. Biol. 236 (2010) 117–125.
[40] V. Regnier, T. Le Doan, V. Preat, Parameters controlling topical delivery of oligonucleotides by electroporation, J. Drug Target. 5 (1998) 275–289.
[41] C. Lombry, N. Dujardin, V. Preat, Transdermal delivery of macromolecules using skin electroporation, Pharm. Res. 17 (2000) 32–37.
[42] M.R. Prausnitz, U. Pliquett, R. Langer, J.C. Weaver, Rapid temporal control of transdermal drug delivery by electroporation, Pharm. Res. 11 (1994) 1834–1837.
[43] T. Jarm, M. Cemazar, D. Miklavcic, G. Sersa, Antivascular effects of electrochemotherapy: implications in treatment of bleeding metastases, Expert. Rev. Anticancer. Ther. 10 (2010) 729–746.
[44] B. Markelc, G. Sersa, M. Cemazar, Differential mechanisms associated with vascular disrupting action of electrochemotherapy: intravital microscopy on the level of single normal and tumor blood vessels, PLoS One 8 (2013) e59557.
[45] J. Gehl, T. Skovsgaard, L.M. Mir, Vascular reactions to *in vivo* electroporation: characterization and consequences for drug and gene delivery, Biochim. Biophys. Acta 1569 (2002) 51–58.
[46] E. Bellard, B. Markelc, S. Pelofy, F. Le Guerroue, G. Sersa, J. Teissie, M. Cemazar, M. Golzio, Intravital microscopy at the single vessel level brings new insights of vascular modification mechanisms induced by electropermeabilization, J. Control. Release 163 (2012) 396–403.
[47] G. Sersa, M. Cemazar, C.S. Parkins, D.J. Chaplin, Tumour blood flow changes induced by application of electric pulses, Eur. J. Cancer 35 (1999) 672–677.
[48] B. Markelc, E. Bellard, G. Sersa, S. Pelofy, J. Teissie, A. Coer, M. Golzio, M. Cemazar, *In vivo* molecular imaging and histological analysis of changes induced by electric pulses used for plasmid DNA electrotransfer to the skin: a study in a dorsal window chamber in mice, J. Membr. Biol. 245 (2012) 545–554.
[49] R. Vanbever, G. Langers, S. Montmayeur, V. Preat, Transdermal delivery of fentanyl: rapid onset of analgesia using skin electroporation, J. Control. Release 50 (1998) 225–235.
[50] C. Herkenne, I. Alberti, A. Naik, Y.N. Kalia, F.X. Mathy, V. Preat, R.H. Guy, *In vivo* methods for the assessment of topical drug bioavailability, Pharm. Res. 25 (2008) 87–103.
[51] J. Schindelin, I. Arganda-Carreras, E. Frise, V. Kaynig, M. Longair, T. Pietzsch, S. Preibisch, C. Rueden, S. Saalfeld, B. Schmid, J.Y. Tinevez, D.J. White, V. Hartenstein, K. Eliceiri, P. Tomancak, A. Cardona, Fiji: an open-source platform for biological-image analysis, Nat. Methods 9 (2012) 676–682.
[52] J.J. Escobar-Chavez, D. Bonilla-Martinez, M.A. Villegas-Gonzalez, E. Molina-Trinidad, N. Casas-Alancaster, A.L. Revilla-Vazquez, Microneedles: a valuable physical enhancer to increase transdermal drug delivery, J. Clin. Pharmacol. 51 (2011) 964–977.
[53] R. Vanbever, E. LeBoulenge, V. Preat, Transdermal delivery of fentanyl by electroporation. I. Influence of electrical factors, Pharm. Res. 13 (1996) 559–565.
[54] R. Vanbever, N.D. Morre, V. Preat, Transdermal delivery of fentanyl by electroporation. II. Mechanisms involved in drug transport, Pharm. Res. 13 (1996) 1360–1366.
[55] M.R. Prausnitz, V.G. Bose, R. Langer, J.C. Weaver, Electroporation of mammalian skin: a mechanism to enhance transdermal drug delivery, Proc. Natl. Acad. Sci. U. S. A. 90 (1993) 10504–10508.
[56] T.W. Wong, T.Y. Chen, C.C. Huang, J.C. Tsai, S.W. Hui, Painless skin electroporation as a novel way for insulin delivery, Diabetes Technol. Ther. 13 (2011) 929–935.
[57] P.Y. Lee, S. Chesnoy, L. Huang, Electroporatic delivery of TGF-beta1 gene works synergistically with electric therapy to enhance diabetic wound healing in db/db mice, J. Invest. Dermatol. 123 (2004) 791–798.
[58] B. Ferraro, Y.L. Cruz, D. Coppola, R. Heller, Intradermal delivery of plasmid VEGF(165) by electroporation promotes wound healing, Mol. Ther. 17 (2009) 651–657.
[59] B. Ferraro, Y.L. Cruz, M. Baldwin, D. Coppola, R. Heller, Increased perfusion and angiogenesis in a hindlimb ischemia model with plasmid FGF-2 delivered by noninvasive electroporation, Gene Ther. 17 (2010) 763–769.
[60] A. Gothelf, P. Hojman, J. Gehl, Therapeutic levels of erythropoietin (EPO) achieved after gene electrotransfer to skin in mice, Gene Ther. 17 (2010) 1077–1084.
[61] B. Ferraro, L.C. Heller, Y.L. Cruz, S. Guo, A. Donate, R. Heller, Evaluation of delivery conditions for cutaneous plasmid electrotransfer using a multielectrode array, Gene Ther. 18 (2011) 496–500.
[62] S. Guo, A. Donate, G. Basu, C. Lundberg, L. Heller, R. Heller, Electro-gene transfer to skin using a noninvasive multielectrode array, J. Control. Release 151 (2011) 256–262.
[63] S. Guo, A.L. Israel, G. Basu, A. Donate, R. Heller, Topical gene electrotransfer to the epidermis of hairless guinea pig by non-invasive multielectrode array, PLoS One 8 (2013) e73432.
[64] K.E. Broderick, X. Shen, J. Soderholm, F. Lin, J. McCoy, A.S. Khan, J. Yan, M.P. Morrow, A. Patel, G.P. Kobinger, S. Kemmerrer, D.B. Weiner, N.Y. Sardesai, Prototype development and preclinical immunogenicity analysis of a novel minimally invasive electroporation device, Gene Ther. 18 (2011) 258–265.
[65] A.K. Roos, F. Eriksson, J.A. Timmons, J. Gerhardt, U. Nyman, L. Gudmundsdotter, A. Brave, B. Wahren, P. Pisa, Skin electroporation: effects on transgene expression, DNA persistence and local tissue environment, PLoS One 4 (2009) e7226.
[66] C. Kanthou, S. Kranjc, G. Sersa, G. Tozer, A. Zupanic, M. Cemazar, The endothelial cytoskeleton as a target of electroporation-based therapies, Mol. Cancer Ther. 5 (2006) 3145–3152.
[67] B. Godin, E. Touitou, Transdermal skin delivery: predictions for humans from *in vivo*, *ex vivo* and animal models, Adv. Drug Delivery Rev. 59 (2007) 1152–1161.
[68] S. Babiuk, M.E. Baca-Estrada, M. Foldvari, L. Baizer, R. Stout, M. Storms, D. Rabussay, G. Widera, L. Babiuk, Needle-free topical electroporation improves gene expression from plasmids administered in porcine skin, Mol. Ther. 8 (2003) 992–998.
[69] L.C. Heller, M.J. Jaroszeski, D. Coppola, A.N. McCray, J. Hickey, R. Heller, Optimization of cutaneous electrically mediated plasmid DNA delivery using novel electrode, Gene Ther. 14 (2007) 275–280.